

On the Breaking of Carbon Nanotubes under Tension

M. A. L. Marques,^{*†} H. E. Troiani,[‡] M. Miki-Yoshida,[§] M. Jose-Yacaman,^{||} and A. Rubio[⊥]

Institut für Theoretische Physik, Freie Universität Berlin, Arnimallee 14, D-14195 Berlin, Germany, Centro Atómico Bariloche (8400), San Carlos de Bariloche, Argentina, Centro de Investigación en Materiales Avanzados, Miguel de Cervantes 120, Chihuahua, Chih., CP 31109, México, Texas Materials Institute and Department of Chemical Engineering, University of Texas at Austin, Austin, Texas 78712, and Departamento de Física de Materiales, UPV/EHU, Centro Mixto CSIC–UPV/EHU, and DIPC, 20018 San Sebastián, Spain

Received January 27, 2004; Revised Manuscript Received March 6, 2004

ABSTRACT

Molecular dynamics simulations and high resolution TEM experiments are performed to assess the fracture of nanotubes under high stretching conditions. Brittle or plastic response is controlled by the rate of applied strain to the tube as well as by the number of defects (in particular vacancies). Simulations predict that under high temperatures and presence of defects (as induced under the high-energy electron beam of the TEM) the tubes exhibit mainly plastic deformation, with the appearance of medium size carbon chains as the latest stage before fracture. These results are in agreement with in-situ TEM observation. Carbon exhibits a very rich dynamics of bond-breaking and bond-reconstruction that allows transformations from fullerenes to tubes to chains.

Carbon nanotubes are indubitably one of the most interesting materials that have been discovered in the past years.¹ They possess extraordinary mechanical (and also electronic) properties, which make them probable building blocks of future high-stiffness materials and molecular nanodevices.² The inherent strength of the carbon–carbon bond indicates that the tensile strength of carbon nanotubes (Young modulus of ~ 1 TPa^{3–5}) might exceed that of other known fibers. In this article we are interested in how nanotubes behave under tensile stress. In ref 4, the nonlinear response of a tube under high strain was studied. Our results build on those studies and provide further insight about the role of defects and temperature on the extraordinary ability of nanotubes to endure large elongations before exhibiting any signal of undergoing bond-breaking or bond-rearrangement.

In a previous work⁶ we used a novel method to generate carbon nanotubes and to study their breaking mechanism under tension. The experiments were performed in a high-resolution transmission electron microscope (HRTEM, JEOL 2010F) equipped with a field emission gun. To directly address the in-situ mechanical dynamics of the tubes we used

the following approach. First, two holes are opened in a initially amorphous ultrathin carbon film with the aid of an intense electron beam. A carbon fiber (i.e., a multiwall carbon nanotube, MWCNT) is formed between the holes and subsequently thins by condensations of the electron beam on specific zones. This process constitutes dramatic evidence of the reconstructive property of carbon bonds under the influence of a high energy electron beam (as already observed in sp²–sp³ transformation and coalescence of carbon nanostructures⁷). At several stages of the thinning process the fiber is not able to sustain the applied tension any longer and breaks in several zones, undergoing structural reconstruction to longer and smaller diameter fibers. This necking mechanism turns out to be an efficient method to release the axial tension in the fiber. This fact is illustrated in the sequence of images in Figure 1. The disruptive/reconstructive behavior of the fiber is observed many times along a breaking experiment until a single wall carbon nanotube (SWCNT) is obtained⁶ (see Figure 1e). At the same time the tendency of the holes to enlarge leads to a net force that stresses even further the carbon fiber. Two failure mechanisms were identified: brittle failure and plastic yielding.⁴ In the former case the fracture occurs before any plastic deformation. Usually, the two nanotube fragments are then closed by fullerene-type caps (see Figure 1f). On the other hand, the ductile SWCNTs undergo a process of necking (which is

* Corresponding author. E-mail: marques@tddft.org.

† Freie Universität Berlin.

‡ Centro Atómico Bariloche.

§ Centro de Investigación en Materiales Avanzados.

|| University of Texas at Austin.

⊥ UPV/EHU.

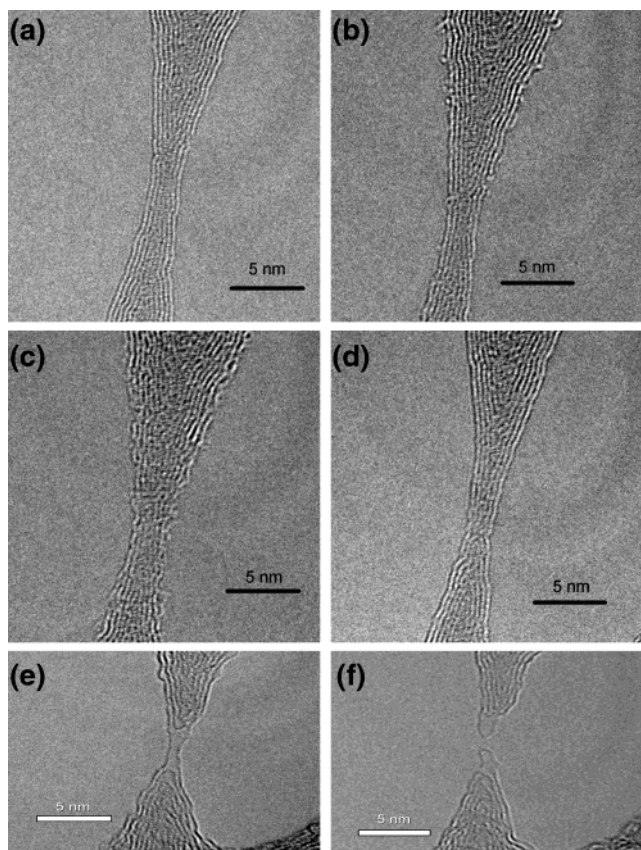


Figure 1. Sequence of high-resolution TEM images detailing the reconstructive properties of carbon under tensile strain. (a) Initial state where all the fiber is in an ordered graphitic state. (b) Beginning of the disruption of the fiber in a region far from thinnest part of the fiber. (c) Complete disruption of the fiber. (d) Reformation of the fiber into a new ordered state with smaller diameter. The sequence a–d appears several times during a tension experiment. (e) A SWCNT is formed as the ultimate product of the thinning process. (f) Breaking of the SWCNT and subsequent capping.

also observed in metallic nanowires⁷). Ultimately some of the tubes deform into a single chain of carbon atoms, spanning the two nanotube ends before fracture.⁶ The character of the bonds in the linear chain was found to be cumulene-type, i.e., with all nearly equivalent bond lengths.

Below, we present an extensive set of simulations which, together with experimental results, allows us to understand the breaking properties of SWCNTs under tension. In particular, we studied the effect of defects, temperature, etc. while stretching the nanotubes. These simulations give a justification for some very interesting properties observed in the HRTEM experiments, like the impressive elastic range of SWCNTs, i.e., the ability of the tube to elongate up to 50% of its length.^{4,6} Both simulations and experimental evidence suggest the ability of nanotubes to significantly change their shape. They develop kinks or ripples (multiwall tubes) in compression and bending, flatten into deflated ribbons under torsion, and still can reversibly restore their original shape.⁸ This resilience is unexpected for a graphite-like material. It must be attributed to the small dimension of the tubules, which leaves no room for stress-concentrators, microcracks, or dislocation piles.

In what concerns technical details, we treat carbon nanotubes as periodic one-dimensional systems. The unit cells are large enough to minimize spurious interaction effects for both single-wall and multiwall tubes. The large number of atoms per unit cell and the long simulation time necessary to describe the breaking procedure (of the order of 100 ps) render impractical the use of fully ab initio methods. To circumvent this problem we used tight-binding, as implemented in our home-grown program⁹ using the parametrization of ref 10. Tight-binding gives a good compromise between precision and computational time. Moreover, and in contrast to methods based on classical potentials, it retains the quantum nature of the electrons. This is fundamental to describe the richness and diversity of bonds in carbon materials, in particular bond-breaking and reconstruction processes occurring during the tensile experiments.

The simulations were performed in the following way. (a) We start by generating a perfect carbon nanotube. (b) If required, defects, like Stone–Wales¹¹ defects or vacancies, are introduced in the tube. (c) The nanotube is thermalized using a Nosé–Hoover thermostat.¹² (d) The tube is stretched by increasing the lattice parameter in the axial direction at constant velocity, v_{stretch} . We have performed this last step in two different regimes, either with a thermostat¹² or without. (e) Steps (c) and (d) are repeated (typically 10 times) to gather statistics on the breaking process.

We note that under the experimental conditions the elongation process does not occur exactly at constant temperature. In fact, at the beginning of the experiment, the tube is in thermal equilibrium with the supporting fiber. If the stretching is slow enough, this situation is maintained until breaking or plastic deformation starts to occur. At this point, the drop in potential energy makes the temperature of the tube rise very steeply. The excess kinetic energy in the region just deformed then propagates through the tube and to the fiber, until the whole system again reaches thermal equilibrium. From these considerations, it is clear that only by combining the two kinds of simulations will it be possible to completely understand the experimental data.

We performed simulations for three prototype tube configurations: the metallic (4,4) tube, the zigzag (4,0), and the double-wall (4,0)@(13,0) tube.¹³ The tubes are described using the following supercells: (a) 5 unit cells of a (4,4) tube, (b) 7 unit cells of the very small (4,0) tube, and (c) 3 unit cells of the double-wall tube (4,0)@(13,0). We deliberately focused on very small diameter tubes for two reasons: (i) small diameter tubes appear at the end of the breaking process of the carbon fiber,⁶ and (ii) recently tubes with $(4 \pm 0.2 \text{ \AA})$ diameter have been synthesized both free-standing and inside the channels of a zeolite matrix.¹⁴ These tubes are mechanically stable up to high temperatures¹⁵ and allow for a direct check of the results presented in this article. To simplify our presentation, we will first show the results for the simulations with the thermostat and then the results without the thermostat.

In Figure 2 we show the result of one of the runs obtained by stretching a perfect (4,4) nanotube at 1500 K. In this simulation the lattice constant was increased at 0.0626 \AA

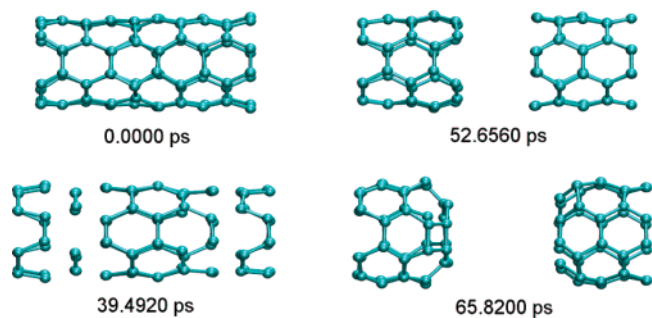


Figure 2. Simulation at 1500 K of the breaking of a (4,4) tube. The sequence shows the nanotube in the equilibrium geometry, breaking of the tube, and capping by fullerene-like structures. Note that “bonds” between atoms are drawn if atoms are closer than 1.7 Å and should not be interpreted as real chemical bonds.

ps^{-1} for a propagation time of around 100 ps. This is a fairly small stretching velocity and is comparable to the thermal vibrations of the carbon atoms at 1500 K. The stretching process occurs in different stages. At the beginning there is a uniform increase of the carbon–carbon bond length. The carbon atoms remain in their hexagonal arrangement, and no defects appear in the structure. This is the situation until $t \sim 50\text{--}58$ ps (depending on the initial conditions), which corresponds to a maximum increase of 30% of the tube length. At this moment the tube breaks and the two fragments contract until the carbon bonds return to their average equilibrium length. This clean cleavage can be justified by the simulation time, too short for the spontaneous formation of defects, and by the small diameter of the tubes that favors the direct bond-breaking dynamics to the creation of defects due to the strong $\pi\text{--}\sigma$ hybridization. (Under high strain and low-temperature conditions, all tubes are brittle. If, on the contrary, external conditions favor plastic flow, such as low strain and high temperature, tubes of diameter less than 1.1 nm show a completely ductile behavior, while larger tubes are moderately or completely brittle depending on their symmetry.⁴) Note that the potential energy released during the contraction process is absorbed by the thermostat. The extremities of the fragments then usually close in a fullerene-like arrangement. The capping process is faster if the extremities of the fragments contain defects that help to decrease the curvature strain (cf. Figure 1f).

The next step is to study how these results change upon introduction of defects. We therefore included either a vacancy or a Stone–Wales¹¹ defect and repeated the calculations. The presence of vacancies can be justified if we think in two different factors: radiation damage and stretching velocity. (a) Radiation damage—vacancies can be created by the removal of atoms from equilibrium positions due to the action of the electron beam inside the microscope. (b) Stretching velocity—if the stretching velocity is too fast, the atoms cannot adjust their positions to the equilibrium conditions.

In most of the simulations (5 out of 11 for the tube with one vacancy and 7 out of 10 for the tube with the Stone–Wales defect) the tube breaks as in the case of perfect tubes. However, in the other cases we observed the formation of a single or a double wire, or even more complicated structures,

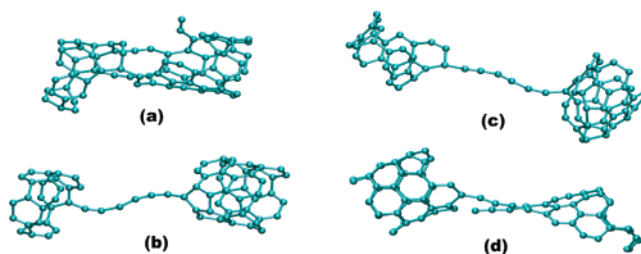


Figure 3. Several structures obtained by stretching a (4,0) nanotube with a Stone–Wales defect (left) or a vacancy (right).

between the tube fragments. Some selected snapshots of these runs are shown in Figure 3. Note that in Figure 3a there is an apparent reduction of the diameter of the tube, which we take as an evidence of the observed necking effect⁶ (see Figure 1). By measuring the time necessary to break the tubes, one can measure the structural weakening due to insertion of defects. The tubes with a Stone–Wales defect break in around 50 ps (after a 25% increase of the tube length), while the tubes with a vacancy break in an average of 42 ps (21% increase). This structural weakening seems to be important for the synthesis of carbon wires.⁴

We also looked at the effect of increasing the stretching velocity. By increasing v_{stretch} to $0.125 \text{ \AA ps}^{-1}$ we obtained carbon wires in 3 runs out of 10. In one case we observe the ejection of a C_2 fragment. At $v_{\text{stretch}} = 0.251 \text{ \AA ps}^{-1}$ we obtained wires in 4 runs out of 10, one of which had a remarkable length of 12 atoms. Finally, at $v_{\text{stretch}} = 0.501 \text{ \AA ps}^{-1}$, only in one case a wire was formed. This nonlinear mechanical response of the carbon nanostructure is relevant to understand the experimental results, as there is a likely correlation between the irradiation dose in the TEM and the appearance of brittle fracture instead of plastic. The velocity of stretching should be in correlation with the time needed to “stabilize” a vacancy during the knock-out collision process with the incoming electron beam in the TEM.

Finally, we performed simulations of (4,4) nanotubes with a vacancy at 320 K (the temperature at which the experiments were performed). Surprisingly, at $v_{\text{stretch}} = 0.125 \text{ \AA ps}^{-1}$, all our runs led to a breaking of the tube (remember that at 1500 K we had obtained 3 wires out of 10 runs). In these conditions, the tube breaks at around $t \sim 25\text{--}30$ ps, which amounts to an increase in length between 25% and 30%. This agrees with the results of ref 4 where it was concluded that all tubes are brittle at high strain and low temperatures.

We also performed simulations without the thermostat. In these, we first thermalized the tube at 320 K and then propagated the Newton equations of motion via a simple Verlet algorithm.¹² For a perfect (4,4) tube, at a stretching velocity of $0.125 \text{ \AA ps}^{-1}$, all runs yielded a uniform expansion for ~ 40 ps (40% increase in length), after which the tube breaks and starts contracting rapidly. In Figure 4 we show how the potential energy rises steadily with the stretching until the tube breaks. The subsequent contraction of the carbon–carbon bonds leads to a sudden decrease of potential energy, and to a steep rise of the temperature to 8000–14000 K. The effect is so violent and localized in the carbon lattice that it sometimes leads to a spectacular

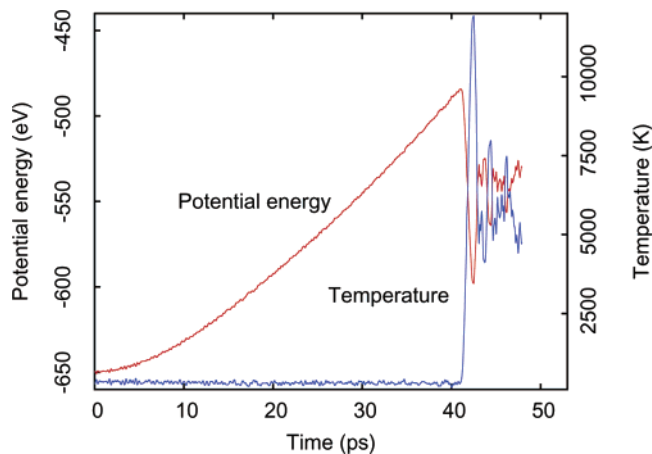


Figure 4. Potential energy and temperature versus time for the MD simulation of the stretching of a perfect (4,4) tube.



Figure 5. Figure of a fourteen atom wire formed by stretching a (4,0) tube containing two vacancies. One can also observe a six atom chain that detached from the tube.

destruction of the tube with ejection of several C_2 fragments. Including a Stone–Wales defect did not change the tube dynamics. However, a structural weakening is evident by looking at the temperature of the system shortly after breaking: around 5000 K. Despite the high temperature, it was still possible to observe the formation of some short-lived wires.

The situation is quite different if we introduce one or more vacancies in the nanotube, as it is expected to occur under electron irradiation in the TEM microscope. In this case, the temperature rises to 2500–4000 K, which apparently is low enough to allow for the formation of wires between the two fragments of the nanotube. At $v_{\text{stretch}} = 0.125 \text{ \AA ps}^{-1}$ we observed the formation of wires in 3 out of 10 runs, and at $v_{\text{stretch}} = 0.0626 \text{ \AA ps}^{-1}$ wires were created in 7 out of 10 runs. We repeated this last run, but starting at 1500 K, and found that in most of the runs a wire was formed, but, due to the higher temperature, the tube underwent fairly large deformations.

Similar results were obtained for the (4,0) tube. It expands for around 34 ps, (34% increase in length), and then breaks and collapses violently. Introduction of one vacancy in the structure leads to the formation of wires in 2 runs out of 10. The production of wires can however be enhanced by the introduction of more vacancies in the structure. By increasing the number of the vacancies to two, we were able to produce very long wires, an example of which is shown in Figure 5. The dynamics of the multiwall tube¹³ are very similar to the ones already described, with the additional formation of intermediate intertube bonds.

In general, while graphite is brittle, carbon nanotubes can exhibit plastic or brittle behavior under deformation, depend-

ing on the external conditions and tube symmetry.⁴ The apparent flexibility stems from the ability of the sp^2 network to rehybridize when deformed out of plane, the degree of sp^2 – sp^3 rehybridization being proportional to the local curvature. (There is accumulated evidence that suggests that the strength of the carbon–carbon bond does not guarantee resistance to radial deformations. In fact, the graphitic sheets of the nanotubes, though difficult to stretch, are easy to bend and to deform.¹) In the simulations, the high strain rate test proceeds in a very peculiar manner. Fast stretching simply elongates the hexagons in the tube wall, until at the critical point an atomic disorder suddenly nucleates: one or a few C–C bonds break almost simultaneously, and the resulting “hole” becomes a crack precursor. The fracture propagates very quickly along the circumference of the tube. A further stage of fracture displays the formation of two or more distinct chains of atoms. The formation of the chain is similar to that observed in the formation and fragmentation of C_{60} .¹⁶ The vigorous motion (substantially above the thermal level) results in frequent collisions between the chains, and soon only one chain survives. A further increase of the distance between the tube ends does not break this chain, which elongates by increasing the number of carbon atoms that pop out from both sides into the necklace. This scenario is similar to the monatomic chain unraveling suggested in field-emission experiments,¹⁷ where the electrostatic force unravels the tube like the sleeve of a sweater. Notably, the breaking varies with temperature, defect concentration and strain rate.

Our simulations show the important role of the vacancies in the plastic dynamics of necking and ulterior thinning of the nanotube, leading ultimately to the formation of (long) linear carbon chains. This plastic response is observed in situations where an otherwise perfect nanotube would undergo brittle fracture.⁴ The picture that emerges from the simulations agrees well with experiments. The fact that the simulations show breaking modes with the presence of linear chains highlights two aspects: that tube breaking proceeds in a high-temperature zone and that the carbon structure is unable of evacuating the heat fast. The region of high temperature is produced by the intense irradiation used to build the tube itself. The impressive elastic range of this structure is understood in terms of the very high Young modulus of the tube that amounts for a uniform distribution of the applied strain and avoids the appearance of crack centers until very high elongation is achieved. The concept of structural weakening due to in-situ created defects in nanotubes is very appealing for applications.⁷ It points a clear direction to follow if one is interested in the synthesis of nanotubes with specific mechanical properties.

Acknowledgment. This work was supported by the EC RTNs NANOPHASE (HPRN-CT-2000-00167), COMELCAN (HPRN-CT-2000-00128), EXC!TING (HPRN-CT-2002-00317), by Spanish MCyT (MAT2001-0946) and University of the Basque Country (9/UPV 00206.215-13639/2001).

References

- (1) Dresselhaus, M. S., Dresselhaus, G., Avouris, Ph., Eds.; *Carbon nanotubes: synthesis, structure, properties, and applications*; Springer-Verlag: Berlin, Heidelberg, 2001.
- (2) Baughman, R. H.; Zakhidov, A. A.; de Heer, W. A. *Science* **2002**, *297*, 787, and references therein.
- (3) See, e.g., Salvetat-Delmotte, J.-P.; Rubio, A. *Carbon* **2002**, *40*, 1729, and references therein.
- (4) Yakobson, B. I. et al., *Comput. Mater. Sci.* **1997**, *8*, 341. Nardelli, M. B.; Yakobson, B. I.; Bernhold, J. *Phys. Rev. Lett.* **1998**, *81*, 4656. Nardelli, M. B.; Yakobson, B. I.; Bernhold, J. *Phys. Rev. B* **1998**, *57*, 4277. Zhang, P.; Lammert, P. E.; Crespi, V. H. *Phys. Rev. Lett.* **1998**, *81*, 5346.
- (5) Lu, J. P. *Phys. Rev. Lett.* **1997**, *79*, 1297. Hernandez, E.; Goze, C.; Bernier, P.; Rubio, A. *Phys. Rev. Lett.* **1998**, *20*, 80.
- (6) H. E. Troiani et al. *Nano Lett.* **2003**, *3*, 751.
- (7) Banhart, F. *Rep. Prog. Phys.* **1999**, *62*, 1181, and references therein. Landman, U.; et al. *Science* **1990**, *248*, 454. Agrat, N.; Rodrigo, J. G.; Vieira, S. *Phys. Rev. B* **1993**, *47*, 12345. Rodrigues, V. et al. *Phys. Rev. B* **2002**, *65*, 153402.
- (8) Iijima, S. et al.; *J. Chem. Phys.* **1996**, *104*, 2089. Falvo, M. R. et al., *Nature* **1997**, *389*, 582.
- (9) This program is free software and can be downloaded from the web page <http://www.tddft.org/programs/octopus/>.
- (10) Xu C. H. et al. *J. Phys. Condens. Matter* **1992**, *4*, 6047. This parametrization not only reproduces well the binding energies and bond lengths of crystalline carbon with different coordination numbers, but also systems such as microclusters and liquid and amorphous carbon.
- (11) Stone, A. J.; Wales, D. J. *Chem. Phys. Lett.* **1986**, *128*, 501.
- (12) Frenkel, D.; Smit, B. *Understanding Molecular Simulations*; Academic Press: San Diego, 1996.
- (13) An analysis of each run, together with plots and movies, can be found in our web site <http://www.tddft.org/tubes/>.
- (14) Qin, L. C. et al. *Nature* **2000**, *408*, 50. Wang, N. et al. *Nature* **2000**, *408*, 50. Hayashi, T., et al. *Nano Lett.* **2003**, *3*, 887.
- (15) Peng, L.-M. et al. *Phys. Rev. Lett.* **2000**, *85*, 3249. Also, the possibility of having sp^3 network in this low diameter tubes has been explored in Stojkovic, D.; Zhang, P.; Crespi, V. H. *Phys. Rev. Lett.* **2001**, *87*, 125502.
- (16) Chelikowsky, J. R. *Phys. Rev. Lett.* **1991**, *67*, 2970.
- (17) Rinzler, A. G., et al. *Science* **1995**, *269*, 1550.

NL049839T